Analysis of 3-Body Angular Momentum States in $\pi N \to \pi\pi N$§

J. M. NAMYSLOWSKI†
Institute of Theoretical Physics and Department of Physics, Stanford University, Stanford, California

AND

M. S. K. RAZMI‡
Tait Institute of Mathematical Physics, University of Edinburgh, Edinburgh, Scotland

AND

R. G. ROBERTS*
Department of Theoretical Physics, Imperial College, London, England

(Received 28 December 1966)

A relativistic formalism for analyzing 3-body angular momentum states in production processes is presented in detail together with examples of several processes $\pi N \to \pi\pi N$ at different energies below 1 BeV. In the final state we assume either one or several 3-particle angular momentum states, belonging to only *one* complete set of states. This enables us to distinguish clearly between different partial-wave transitions, and to make our analysis in a systematic way. As a dynamical assumption we use the isobar model, and allow only a minimum number of transitions in order to minimize the number of free parameters. Our formulas are written in terms of variables used in the Faddeev theory with separable approximation; thus they can be applied for testing solutions of the Faddeev equation.

I. INTRODUCTION

THE present paper is an extension of the formalism proposed earlier.[1] Here, we make an attempt to analyze 3-body angular momentum states in several production processes. The $\pi\pi N$ system is used to present details of calculations. We summarize in Sec. II different methods of partial-wave analysis of 2- $\to$ 3-body transitions. The emphasis is put on the necessity of using only *one* complete set of the 3-particle angular momentum states in the final state. It is especially important if several transitions have to be included, and the analysis is to be made in a systematic way.

In Sec. III we present our angular and isospin decompositions. We use two unit operators made up from the 3-particle angular momentum states, and one unit operator formed by the 2-particle angular momentum states. That enables us to discuss transitions from a given initial 2-body angular momentum state to a given final 3-body angular momentum state belonging to only one complete set of states.

Section IV, together with Appendix A, contains the necessary formulas for calculating the mass and angular distributions. These formulas are based on our angular and isospin decompositions, and are expressed in terms of the radial parts of partial-wave transitions. To calculate these radial parts we make a dynamical approximation, assuming the isobar model. This is presented in Sec. V, where we write formulas, using the notation of the Faddeev theory in the separable approximation, discussed by Freedman, Lovelace, and Namyslowski.[2] Our formalism can be used for testing solutions of the 3-particle Faddeev equations, when they are solved.

Using the assumption of the isobar model, we present in Sec. VI the partial-wave analysis for several processes $\pi N \to \pi\pi N$, at different energies, below 1 BeV. We normalize the calculated distribution to the same area as the experimental histogram. Our results should be considered only as an example of the analysis of the 3-body angular momentum states. We have tried to explain several collections of experimental data, using a minimum number of partial-wave transitions, which were compatible with the data. The requirement of the smallest number of transitions was imposed, to minimize the number of free parameters, which are unavoidable in a dynamical model. A more extensive analysis will be possible when a solution of the dynamical theory, like the Faddeev equations is obtained. Our formalism is written in variables used in the separable approximation of the Faddeev theory; thus it is ready for further applications.

In Sec. VII we compare our approach with several other formalisms.

II. DIFFERENT METHODS OF PARTIAL-WAVE ANALYSIS IN THE $\pi\pi N$ SYSTEM

To make a partial-wave analysis one has to work with states of angular momentum. Such states, for the

§ Supported in part by AFOSR contract AF49(638)-1389.
† On leave from Jagellonian University, Cracow, Poland.
‡ Present address: Department of Physics, University of Toronto, Toronto, Canada.
* Present address: Department of Physics, University of Durham, Durham City, England.
[1] J. M. Namyslowski, M. S. K. Razmi, and R. G. Roberts, Imperial College, London, Report No. ICTP/65/20, 1965 (unpublished).
[2] D. Z. Freedman, C. Lovelace, and J. M. Namyslowski, Nuovo Cimento 43, 258 (1966).

3-particle system, can be defined in various ways.[3–8] In some of them,[3,4] we first combine a pair of particles into a system, and then, in turn, consider this system and the third particle. Of course by doing that in all possible ways we get three independent complete sets of angular momentum states. Other methods[5,6] employ so-called "rigid-body" partial-wave amplitudes, and have only one set of angular momentum states. Yet, there are other methods[7,8] which also use one set of angular momentum states, but differ from the previous one by using different additional quantum numbers, besides the total angular momentum and its projection. Such variety of 3-particle angular momentum states in itself produces different ways of classifying partial-wave amplitudes of the production processes. However, besides having different tools for the partial-wave analysis, we can also consider different methods of using them, especially in the $\pi\pi N$ system. We shall discuss three of these methods, which have already been used: (1) Angular momentum states form only one set of states.[9] (2) Several independent sets of angular momentum states are used, and in the final state there is allowed a combination of states from two different sets.[10,11] (3) Several independent sets are used, but in the final state there is either one, or several angular momentum states, which always belong to the same set.[1]

The first method is the most straightforward one and, as was shown by Arnold and Uretsky,[9] it can be used for getting some restrictions on the total angular momentum of the whole system. However, to get a more detailed analysis of the final angular momentum states, one has to employ a dynamical model. Such a dynamical model is obtained by assuming production of the N^*, which can be formed from either one of two pions and the nucleon. This dynamical model focuses our attention on the second and third method. Both of them can easily handle simultaneous production of N^* in two channels, $(\pi_1 N)\pi_2$ and $(\pi_2 N)\pi_1$. Comparing that with the first method, one can consider some additional information about the orbital angular momenta, besides the total angular momentum. This new information is generated by a specific dynamical model, but one can use it in several different cases and see how consistently it can explain the $\pi\pi N$ system at different energies.

The second and third methods are similar in exploring the dynamical assumptions of N^* production; however, they differ essentially in formulating the partial-wave analysis. Let us start from the second method and show an example of the final state. For clarity we shall use the canonical base, and denote a state of the 3-particle angular momenta by $|JL_\alpha Sl_\alpha\sigma_\alpha\rangle$, where $\alpha=1, 2, 3$. Pions are denoted by 1, 2, and nucleon by 3. J, S are the total angular momentum and total spin of the $\pi\pi N$ system. L_α is the orbital angular momentum of the particle α in the over-all center-of-mass system. l_α is the orbital angular momentum of the $(\beta\gamma)$ subsystem in the 2-body center-of-mass system. σ_α is the total spin of the $(\beta\gamma)$ subsystem. To account for the simultaneous production of N^* in channels $(\pi_1 N)\pi_2$ and $(\pi_2 N)\pi_1$, one considers the following final state:

$$|JL_1Sl_1\sigma_1\rangle+|JL_2Sl_2\sigma_2\rangle. \tag{1}$$

That state one would be willing to call a given angular momentum state, if we have

$$L_1=L_2, \quad l_1=l_2, \quad \sigma_1=\sigma_2. \tag{2}$$

However, even if we have Eq. (2), we still cannot call Eq. (1) a given angular momentum state. The reason is that each of the components of Eq. (1) belongs to a different, independent set of states. Thus, it can be decomposed into many states of the set where the other state of Eq. (1) belongs. In that sense, within the second method, one cannot define the partial-wave analysis as an analysis of transitions to a definite final 3-body angular momentum state. That difficulty seems at first to be merely a formal one; however, it is more serious if one has to include several angular momentum states. It would be difficult then, by using the second method, to perform a systematic analysis of partial waves. If we would first allow only one wave and later assume a superposition of several of them, then at each step we would be dealing with an infinite collection of the angular momentum states.

This difficulty leads us to investigate the third method, if we would like to take into account several interfering states in a systematic way. The details of the third method, and its application, are presented in the following sections.

The third method, besides avoiding the above-mentioned difficulty, also has a few advantages. It is a more selective method because the final state is specified in more detail. This will become clear from our numerical results which can be compared with results obtained by using the second method. Another advantage of the third method is that it can be extended beyond the isobar model. This would be rather difficult to do in the second method, because we have to assume that Eq. (2) is satisfied in order to get any meaning from the partial-wave analysis.

---

[3] G. C. Wick, Ann. Phys. (N. Y.) **18**, 65 (1962); see also M. Jacob and G. C. Wick, *ibid.* **7**, 404 (1959).
[4] A. J. Macfarlane, J. Math. Phys. **4**, 490 (1963); A. J. Macfarlane, Rev. Mod. Phys. **34**, 41 (1962).
[5] D. Branson, P. V. Landshoff, and J. G. Taylor, Phys. Rev. **132**, 902 (1963).
[6] R. Omnes, Phys. Rev. **134**, B1358 (1964).
[7] J. Werle, Phys. Letters **4**, 128 (1963); Nucl. Phys. **44**, 579 (1963); **44**, 637 (1963); **49**, 433 (1963); **57**, 245 (1964); S. M. Berman and M. Jacob, Phys. Rev. **139**, B1023 (1965).
[8] W. A. Wilson, University of California, San Diego, Report No. UCSD-10P10-5, 1966 (unpublished).
[9] R. C. Arnold and J. L. Uretsky, Phys. Rev. **153**, 1443 (1967).
[10] P. G. Thurnauer, Phys. Rev. Letters **14**, 985 (1965); University of Rochester Report No. UR-875-119, 1966 (unpublished).
[11] B. Deler and G. Valladas, Nuovo Cimento **45A**, 559 (1966).

III. SEPARATION OF ANGULAR AND ISOSPIN DEPENDENCE

A. Angular Dependence

In this section we present a few details of the third method. The basic novelty of it, in comparison with the second method, is the use of two unit operators made up from two complete sets of the 3-particle angular momentum states. One of these unit operators enables us to focus our attention on a particular final state, or on a superposition of states belonging to the same set. The other unit operator is introduced only because of the dynamical model. We can choose this second unit operator to be made up from the most convenient set of states, in order to get the best framework for the dynamical assumption. The recoupling coefficients which show up in the expression for the T-matrix element are well known and can be exactly calculated if we have defined the appropriate set of states. From the above remarks one sees that the third method can be easily used in any dynamical model, simply by choosing the most convenient set for the second unit operator.

Besides the two unit operators formed from the 3-particle states, we also use a unit operator made from the 2-particle angular momentum states. This is for selecting a given angular momentum state of the initial particles. Thus, we can discuss transitions between a definite initial and final angular momentum state.

Let us start from the plane-wave representation of the T matrix, and define the amplitude T by

$$\langle k_\alpha\lambda_\alpha,k_\beta\lambda_\beta,k_\gamma\lambda_\gamma|T|k_a\lambda_a,k_b\lambda_b\rangle = \delta^4(k_\alpha+k_\beta+k_\gamma-k_a-k_b)T_{\lambda_a\lambda_b}{}^{\lambda_\alpha\lambda_\beta\lambda_\gamma}, \quad (3)$$

where $k_\alpha\cdots k_b$ denote momenta of particles, and $\lambda_\alpha\cdots\lambda_b$ are helicities. For the angular momentum representation we use states defined by Wick[3] in the helicity scheme, and by Macfarlane[4] in the canonical base. These two formalisms are compared in McKerrell's[12] paper. Most of our formulas will be presented in the helicity scheme because they are simpler than the results in the canonical base. However, for making a dynamical approximation it is easier to work with the canonical base.

A standard way of extracting the angular part in the T matrix is to rewrite its plane-wave representation in terms of the angular momentum representation. Let us denote, *schematically* the Wick[3] 3-particle angular momentum states by $|\alpha(\beta\gamma)\rangle$, and insert in Eq. (3) two unit operators

$$\sum\sum|\alpha(\beta\gamma)\rangle\langle\alpha(\beta\gamma)|\gamma(\alpha\beta)\rangle\langle\gamma(\alpha\beta)|. \quad (4)$$

Besides Eq. (4), we insert in Eq. (3) one unit operator for initial particles, and get the decomposition of the T matrix which will be denoted by $T(\alpha,\gamma)$ to emphasize two unit operators introduced in Eq. (4). We obtain the following expression:

$$T_{\lambda_a\lambda_b}{}^{\lambda_\alpha\lambda_\beta\lambda_\gamma}(\alpha,\gamma)=\sum_{J\,j_\alpha m_\alpha\nu_\beta\nu_\gamma} 8\left(\frac{W^2w_\alpha}{k_ap_\alpha q_\alpha}\right)^{1/2} N_J{}^2N_{j\alpha}e^{-i\pi(s_\alpha+s_\gamma+s_b)}d_{\lambda_\beta\nu_\beta}{}^{s_\beta}(\beta_{\beta\gamma})d_{\lambda_\gamma\nu_\gamma}{}^{s_\gamma}(\beta_{\gamma\beta})d_{m_\alpha\nu_\beta\gamma}{}^{j_\alpha}(\theta_\alpha)D_{\lambda^0,m_\alpha-\lambda_\alpha}{}^{J*}(s_\alpha)$$
$$\times\left[\sum_{j_\gamma m_\gamma\mu_\alpha\mu_\beta\mu_\gamma}\int dw_\gamma{}^2U_{j_\gamma m_\gamma\mu_\alpha\mu_\beta;\,\mu_\gamma}{}^{j_\alpha m_\alpha\nu_\beta\nu_\gamma;\,\lambda_\alpha}(w_\alpha,w_\gamma)T_{\lambda_a\lambda_b}{}^{J\,j_\gamma m_\gamma\mu_\alpha\mu_\beta;\,\mu_\gamma}(w_\gamma,W)\right], \quad (5)$$

where W, J, M are total energy, angular momentum, and its projection of the whole 3-particle system in the over-all center-of-mass frame. w_α, j_α, m_α are the same as above, for the $(\beta\gamma)$ subsystem. q_α is the relative momentum of the particle α in the over-all center-of-mass system. p_α is the relative momentum in the $(\beta\gamma)$ subsystem. $\beta_{\beta\gamma}\cdots\theta_\alpha$ are angles on the Wick triangle and they are explained in Fig. 1 and in Appendix B. s_α, in the argument of the D function, stands for three Euler angles Θ_α, Φ_α, and φ_α, which are polar and azimuthal angles of $\mathbf{q}_\alpha$ with respect to the overall c.m. system and azimuthal angle of $\mathbf{p}_\alpha$ in the $(\beta\gamma)$ subsystem, respectively. s_α, as the upper index of the d function, denotes the spin of the particle α.

$$U_{j_\gamma m_\gamma\mu_\alpha\mu_\beta;\,\mu_\gamma}{}^{j_\alpha m_\alpha\nu_\beta\nu_\gamma;\,\lambda_\alpha}(w_\alpha,w_\gamma)$$

is the recoupling coefficient, described in Wick's[3] paper by the formula (35), with the additional factor

$$\delta\{\cos\theta_\alpha'-(4Ww_\alpha p_\alpha q_\alpha)^{-1}[(W^2-m_\alpha{}^2)(m_\gamma{}^2-m_\beta{}^2)+w_\alpha{}^2(W^2+m_\alpha{}^2+m_\beta{}^2+m_\gamma{}^2-w_\alpha{}^2)-2w_\alpha{}^2w_\gamma{}^2]\}.$$

To carry out the integration we use the Jacobian

$$\frac{\partial w_\gamma{}^2}{\partial\cos\theta_\alpha'}=\frac{2Wp_\alpha q_\alpha}{w_\alpha}.$$

$T_{\lambda_a\lambda_b}{}^{J\,j_\gamma m_\gamma\mu_\alpha\mu_\beta;\,\mu_\gamma}$ is the radial part of the T-matrix element

$$\langle PJMw_\gamma j_\gamma m_\gamma\mu_\alpha\mu_\beta;\,\mu_\gamma|T|PJM\lambda_\alpha\lambda_\beta\rangle.$$

Finally,

$$N_J\equiv(2J+1/4\pi)^{1/2},\quad \nu_{\beta\gamma}\equiv\nu_\beta-\nu_\gamma,\quad \lambda'\equiv\lambda_a-\lambda_b.$$

Besides Eq. (5) for $T(\alpha,\gamma)$, we shall also use decompositions which will be denoted by $T(\alpha,\beta)$ and $T(\alpha,\alpha)$. Formulas for them are exactly analogous to Eq. (5).

[12] A. McKerrell, Nuovo Cimento **34**, 1289 (1964).

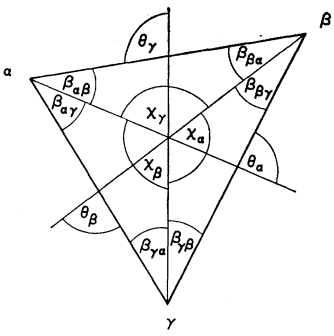

FIG. 1. The Wick triangle. It is a triangle in a non-Euclidean space. For more details see Ref. 3. All angles can be expressed in terms of the total energy W and subenergies w_1, w_2, and w_3. A few examples of such expressions are given in Appendix B.

To write them, one changes notation and takes care of the appropriate phase convention according to Wick's[3] paper. The reason for using all three decompositions $T(\alpha,\alpha)$, $T(\alpha,\beta)$, and $T(\alpha,\gamma)$ is to account for simultaneous production of N^* and/or for two-pion resonances. We shall discuss this in Sec. IV.

To get expressions in the canonical base, from those which were obtained in the helicity representation, we use the inverse of McKerrell's[12] formulas. For the 3-particle angular momentum state we have the following relation:

$$|PJMw_\alpha j_\alpha m_\alpha \lambda_\beta \lambda_\gamma;\lambda_\alpha\rangle=(2w_\alpha)^{-(1/2)}$$
$$\times\sum_{l_\alpha \sigma_\alpha L_\alpha S}\left[\frac{(2L_\alpha+1)(2l_\alpha+1)}{(2J+1)(2j_\alpha+1)}\right]^{1/2} C_{0,m_\alpha-\lambda_\alpha,m_\alpha-\lambda_\alpha}{}^{L_\alpha SJ}$$
$$\times C_{m_\alpha,-\lambda_\alpha,m_\alpha-\lambda_\alpha}{}^{j_\alpha s_\alpha S} C_{0\lambda_\beta\gamma\lambda_\beta\gamma}{}^{l_\alpha\sigma_\alpha i_\alpha} C_{\lambda_\beta,-\lambda_\gamma,\lambda_\beta\gamma}{}^{s_\beta s_\gamma\sigma_\alpha}$$
$$\times|PJML_\alpha S l_\alpha\sigma_\alpha\rangle, \quad (6)$$

where S is the total spin of the 3-particle system; L_α is the relative orbital angular momentum of the system α particle and the $(\beta\gamma)$ subsystem; l_α is the relative angular momentum in the $(\beta\gamma)$ subsystem, and σ_α is the total spin in the $(\beta\gamma)$ subsystem.

B. Isospin Dependence

In the same way as we have extracted the angular dependence, we can find the isospin structure of the T-matrix element. We write

$$T=\langle I_\alpha i_\alpha, I_\beta i_\beta, I_\gamma i_\gamma|T|I_a i_a, I_b i_b\rangle,$$

where $I_\alpha\cdots I_b$ are isospins of the corresponding particles, and $i_\alpha\cdots i_b$ are the z-components of the isospin. By inserting the appropriate unit operators we get

$$T(\alpha,\gamma)=\sum_{I,T_\alpha,T_\gamma}\Lambda_{IT_\alpha}V_{T_\gamma I_\gamma}{}^{I;T_\alpha I_\alpha}T_{I_a I_b}{}^{I;T_\gamma I_\gamma}, \quad (7)$$

where I, T_α are total isospins of three particles, and the $(\beta\gamma)$ subsystem, correspondingly.

$$\Lambda_{IT_\alpha}\equiv C_{i_\beta i_\gamma t_\alpha}{}^{I_\beta I_\gamma T_\alpha} C_{t_\alpha i_\alpha i}{}^{T_\alpha I_\alpha I} C_{i_a i_b i}{}^{I_a I_b I}.$$

We have skipped some indices on the left-hand side to simplify the notation.

$$V_{T_\gamma I_\gamma}{}^{I;T_\alpha I_\alpha}\equiv(-1)^{2I+I_\beta+I_\gamma-T_\alpha}(2T_\alpha+1)^{1/2}$$
$$\times(2T_\gamma+1)^{1/2}\begin{Bmatrix} I_\alpha & I_\beta & T_\gamma \\ I_\gamma & I & T_\alpha\end{Bmatrix},$$

where the final bracket denotes the familiar $6j$ symbol.[13] A similar decomposition, denoted by $T(\alpha,\beta)$ and $T(\alpha,\alpha)$, will be used with Eq. (7).

IV. MASS AND ANGULAR DISTRIBUTIONS

A. Mass Distributions

Let us assume, for a moment, that we know the radial part of the T matrix. We shall discuss in Sec. V some approximate form of the radial part. Using our angular and isospin decompositions of the form of Eqs. (5) and (7), we can write an expression for the T matrix of the process

$$(k_a\lambda_a I_a)+(k_b\lambda_b I_b)\to(k_\alpha\lambda_\alpha I_\alpha)+(k_\beta\lambda_\beta I_\beta)+(k_\gamma\lambda_\gamma I_\gamma). \quad (8)$$

We get

$$T=\tfrac{1}{3}[T(\alpha,\alpha)+T(\alpha,\beta)+T(\alpha,\gamma)]. \quad (9)$$

In Eq. (9) we have used the completeness of each set of Wick[3] states, and have written the expression for the T matrix in a form which guarantees the symmetry property[3,14] required by two bosons in the final state. A similar formula to Eq. (9) is also discussed by Thurnauer,[10] who included more general coefficients in front of each T. However, one should bear in mind the difference between, e.g. $T(\alpha,\beta)$, obtained by using two unit operators of the 3-particle states, and the decomposition used by Thurnauer,[10] where only one unit operator is used for the 3-particle system. It is important that all T's in Eq. (9) have the same first index α, if we wish to have the final state decomposed in terms of *one* complete set of angular momentum states.

To get the differential cross section for the process [Eq. (8)] we denote

$$P(w_\alpha,\theta_\alpha,\Theta_\alpha,\Phi_\alpha,\varphi_\alpha)$$
$$\equiv\sum_{\lambda_\alpha\lambda_\beta\lambda_\gamma\lambda_a\lambda_b}\tfrac{1}{9}|T(\alpha,\alpha)+T(\alpha,\beta)+T(\alpha,\gamma)|^2, \quad (10)$$

so that the cross section is given by

$$d\sigma=\frac{\pi^2}{16F(2s_a+1)(2s_b+1)}\frac{p_\alpha q_\alpha}{Ww_\alpha}P(w_\alpha,\theta_\alpha,\Theta_\alpha,\Phi_\alpha,\varphi_\alpha)$$
$$\times dw_\alpha{}^2 d\cos\theta_\alpha d\varphi_\alpha d\cos\Theta_\alpha d\Phi_\alpha, \quad (11)$$

where

$$F=[(\hat{k}_\alpha\cdot\hat{k}_\beta)^2-m_a{}^2m_b{}^2]^{1/2}.$$

[13] A. R. Edmonds, *Angular Momentum in Quantum Mechanics* (Princeton University Press, Princeton, New Jersey, 1957).
[14] P. Carruthers, Ann. Phys. (N. Y.) **14**, 229 (1961).

From Eq. (11) one can get expressions both for mass and angular distributions. The formula for the mass spectrum is the following:

$$(d\sigma/dw_\alpha^2)=(2\pi)^3[9k_a^2(2s_a+1)(2s_b+1)]^{-1}\times\sum_{\lambda_\alpha\nu_\beta\nu_\gamma\lambda_a\lambda_b}\sum_{J j_\alpha j_{\alpha'} m_\alpha} N_J^2 N_{j_\alpha} N_{j_{\alpha'}}\times\int d\cos\theta_\alpha d_{m_\alpha\nu_\beta\gamma}^{j_\alpha}(\theta_\alpha) d_{m_\alpha\nu_\beta\gamma}^{j_{\alpha'}}(\theta_\alpha)\times M_{\lambda_a\lambda_b}{}^{J j_\alpha m_\alpha\nu_\beta\nu_\gamma\lambda_\alpha} M_{\lambda_a\lambda_b}{}^{J j_{\alpha'} m_\alpha\nu_\beta\nu_\gamma\lambda_\alpha *}, \quad (12)$$

where $M_{\lambda_a\lambda_b}{}^{J j_\alpha m_\alpha\nu_\beta\nu_\gamma\lambda_\alpha}$ is given in Appendix A. M contains the recoupling coefficients in the angular momentum and in isospin space, multiplied by the radial part of the T matrix. In Eq. (12) there is only one integration left for numerical calculation. When doing this integration one has to remember that all angles on the Wick[3] triangle are functions of subenergies, as shown in Appendix B.

B. Angular Distributions

From Eq. (11) we can also get expressions for a different angular distribution. The simplest of them is the production angular distribution at a fixed subenergy $(\partial^2\sigma/\partial w_\alpha^2\partial\cos\Theta_\alpha)$. The formula for it contains only one one-dimensional integral over $\cos\theta_\alpha$.

To calculate the decay angular distribution we have to make a transformation of angles. Our polar angles θ_α, φ_α refer to the z axis in the rest frame of the 2-particle subsystem, which is taken in the direction of $\mathbf{q}_\alpha$. However, it is customary with experimentalists to work with the decay angular distribution which is a function of the polar angles ξ_α, η_α. These angles are measured with respect to the z axis lying in the direction of the momentum $\mathbf{k}_a$, when seen from the rest frame of the 2-particle subsystem. To pass from one frame of reference to the other we have to make a rotation through an angle ζ_α about the y axis, which is common to both systems of reference. One can find the following relation:

$$\cos\zeta_\alpha=\frac{(w_\alpha^2+q_\alpha^2)^{1/2}k_a\cos\Theta_\alpha-q_\alpha k_a{}^0}{\{[q_\alpha k_a\cos\Theta_\alpha-(w_\alpha^2+q_\alpha^2)^{1/2}k_\alpha{}^0]^2-w_\alpha^2 m_\alpha^2\}^{1/2}}. \quad (13)$$

This rotation through the angle ζ_α induces a transformation on the function $P(w_\alpha,\theta_\alpha,\Theta_\alpha,\Phi_\beta,\varphi_\alpha)$, defined by Eq. (10). We can explicitly carry out such transformation on each term in our angular momentum series, using the known transformation properties of D functions.[13] The result is a rather lengthy expression, so instead of writing it we merely add the following remarks. The expression for the decay angular distribution of the 2-particle subsystem, at a fixed subenergy $\partial^2\sigma/\partial w_\alpha^2\partial\cos\xi_\alpha$ contains only one one-dimensional integral over $\cos\Theta_\alpha$. The Treiman-Yang angle distribution, at a fixed subenergy $\partial^2\sigma/\partial w_\alpha^2\partial\eta_\alpha$, contains a product of two one-dimensional integrals, one over $\cos\xi_\alpha$, the other over $\cos\Theta_\alpha$.

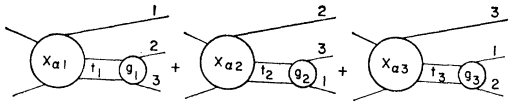

FIG. 2. Graphical representation of Eq. (14).

V. DYNAMICAL APPROXIMATIONS

As a dynamical model we employ the isobar model[15–17] in a form which is used in the separable Faddeev equation presented by Freedman, Lovelace, and Namyslowski.[2] Having our expressions written in the same form as in the Faddeev theory, we can in the future replace the assumption of a model by a solution of the dynamical equation. At present we only test our formulas by using the isobar model.

In the separable Faddeev theory the isobar model is formulated by the following approximation of the radial part of the T matrix:

$$\langle PJML_\alpha Sl_\alpha\sigma_\alpha|T|PJML'S'\rangle\approx\sum_\gamma X_{\alpha\gamma}{}^{JL} t_\gamma g_\gamma, \quad (14)$$

where $X_{\alpha\gamma}{}^{JL}$ is a composite particle scattering amplitude defined in Ref. 2, t_γ is the propagator of the $(\alpha\beta)$ subsystem, and g_γ is a form factor of the $(\alpha\beta)$ subsystem. Graphically we represent the right-hand side of Eq. (14) by Fig. 2.

We assume that each term of Eq. (14) is proportional to the following centrifugal-barrier factors:

$$(q_\gamma/a_\gamma)^{L_\gamma}(p_\gamma/b_\gamma)^{l_\gamma}, \quad (15)$$

where a_γ is the reduced energy of the particle γ and the subsystem $(\alpha\beta)$ in the over-all center-of-mass system. b_γ is the reduced energy of particles α and β in their 2-particle center-of-mass system. In Eq. (15) we do not include a centrifugal-barrier factor coming from the initial state, because at a fixed initial energy it gives only a constant factor. Our calculated distributions will be always normalized to the same area as the experimental histogram.

For the propagator t_γ we take

$$t_\gamma=[w_\gamma-w_0+i\Gamma(w_\gamma)]^{-1}, \quad (16)$$

where w_0, and $\Gamma(w_\gamma)$ are the position and the half-width of a 2-particle resonance. For $\Gamma(w_\gamma)$ we have assumed

[15] S. J. Lindenbaum and R. J. Sternheimer, Phys. Rev. **105**, 1874 (1957); **106**, 1107 (1957); **109**, 1723 (1958).
[16] S. Bergia, F. Bonsignori, and A. Stanghellini, Nuovo Cimento **16**, 1073 (1960).
[17] M. Olsson and G. B. Yodh, Bull. Am. Phys. Soc. **8**, 68 (1963); M. Olsson and G. B. Yodh, Phys. Rev. Letters **10**, 353 (1963); M. Olsson, Ph.D. thesis, University of Maryland, 1964 (unpublished); M. Olsson and G. B. Yodh, Phys. Rev. **145**, 1309 (1966); **145**, 1327 (1966).

the following form:

$$\Gamma(w_\gamma)=\Gamma_0\left(\frac{g_\gamma(w_\gamma)}{g_\gamma(w_0)}\right)^2\frac{p_\gamma}{b_\gamma}. \tag{17}$$

This form of $\Gamma(w_\gamma)$ implies that $\Gamma\sim\Gamma(p_\gamma/p_0)^{2l_\gamma+1}$; thus our assumption [Eq. (17)] is similar to the one used by Jackson.[18]

The isobar model, besides enabling us to write the formula for the radial part of the T matrix, also puts several restrictions on the sums in Eq. (12). By assuming the N^* production we cut the sums over either j_1 or j_2 to only one term, corresponding to $j_1=\frac{3}{2}$ or $j_2=\frac{3}{2}$. We are considering here sums which are connected with the unit operators denoted by β or γ in Eq. (9). These sums correspond to the second unit operator in Eq. (4). The other sums, corresponding to the first unit operator in Eq. (4), are still infinite, and we will discuss them in the next section where the partial-wave analysis is set up.

The validity of the isobar model with the N^* production is restricted to the region where the initial pion beam energy is below 1 BeV. That implies such a range of subenergies w_1, w_2 that the πN cross section is dominated by the $N^*(1238,118)$ resonances.

Considering the $\pi\pi$ subsystem, we shall assume throughout most of our calculations that there is no $\pi\pi$ resonance. Thus, one of the terms in Eq. (14) will drop out. However, there will be one case, at the initial pion-energy of 430 MeV, where we find it necessary to allow some $\sigma(400,50)$ production together with the N^* production. In that case all three graphs of Fig. 2 are included in the dynamical model.

VI. PARTIAL-WAVE ANALYSIS

A. Discussion of Method

According to the usual procedure of the partial-wave analysis we extract from the full amplitude only those

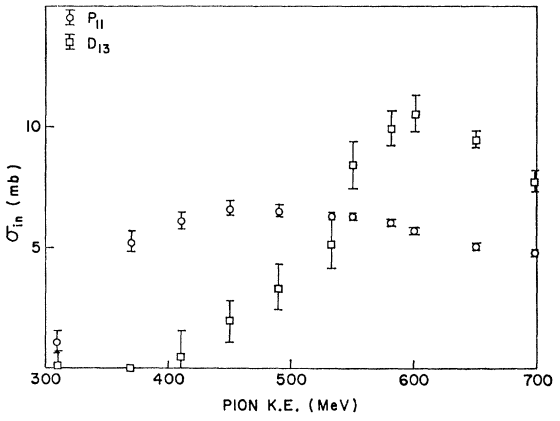

FIG. 3. Partial inelastic cross section in the P_{11} and D_{13} states, obtained from the πN phase-shift analysis of Lovelace *et al.* (Ref. 19).

[18] J. D. Jackson, Nuovo Cimento **34**, 1644 (1964).

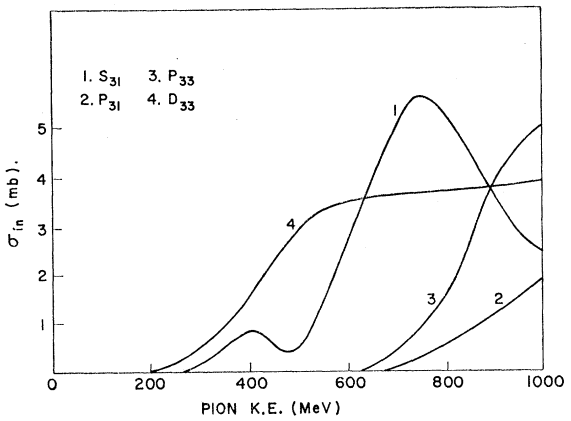

FIG. 4. Partial inelastic cross section in the S_{31}, P_{31}, P_{33}, and D_{33} states, obtained from the results of Donnachie *et al.* (Ref. 20).

partial-wave transitions which are compatible with all available experimental data. We start by assuming that only one transition, from a given initial angular momentum state to a given final angular momentum state, dominates the considered process. If that fails to explain the data, then we try a superposition of several transitions.

The initial angular momentum states are almost uniquely determined. They are 2-particle states; thus we have only one set of angular momentum states. We can use results obtained from the phase-shift analysis for the πN scattering in the inelastic region to extract the most dominant initial states. These results are shown in Figs. 3 and 4. They were obtained by Lovelace *et al.*[19,20] There is an ambiguity which can arise by neglecting transitions corresponding to $J\geqslant\frac{5}{2}$, as it was pointed out by Arnold and Uretsky.[9] We shall, however, stick to the assumption that $J\leqslant\frac{3}{2}$, and in this case we have uniquely determined the initial angular momentum states.

The final angular momentum states are the 3-body states; therefore we can build several independent sets of angular momentum states. To make a systematic partial-wave analysis we have to stick to only one of these sets and not mix states from different sets. Any of the independent sets can be chosen for the final state, because each of them is a complete set. However, some of the experimental data will be easier to classify when working with one particular set. For example, the $\pi\pi$ spectrum will be easiest to discuss in the angular momentum states built up according to the $(\pi\pi)N$ scheme. Besides a formal reason, there is also an essential advantage to use this scheme. Namely, the dynamical assumption is put in the $(\pi N)\pi$ scheme because of the N^* production; thus, when calculating the $\pi\pi$ mass spectrum in the angular momentum state of the $(\pi\pi)N$ scheme, we will integrate over the πN subenergies. In

[19] C. Lovelace, Proc. Roy. Soc. (London) **289A**, 547 (1966).
[20] A. Donnachie, A. T. Lee, and C. Lovelace, Phys. Letters **19**, 146 (1965).

that way we will average over the radial part of the amplitude; therefore the approximate form of it will have rather small effect on the $\pi\pi$ mass spectrum. We have checked it by taking various assumptions for the radial parts. The $\pi\pi$ spectrum was almost unchanged if we were considering the same transition. On the other hand, the $\pi\pi$ mass spectrum is very sensitive to the choice of the angular momentum. Thus it provides a sensitive criterion for the partial-wave analysis even at the stage when the radial part of the amplitude is only roughly approximated.

As well as studying the set of the final angular momentum states in the $(\pi\pi)N$ scheme, it is also interesting to ask which of the lowest angular momentum states are most important in the $(\pi N)\pi$ scheme, where we are making the dynamical assumption. We cannot simply project the state which we obtain in the $(\pi\pi)N$ scheme on the set of states of the $(\pi N)\pi$ scheme. That will give us an infinite number of states and not the lowest one, for which we are looking. It should be remembered that the recoupling coefficients, between states of two sets of the 3-particle angular momentum states, are diagonal only in the total angular momentum and its projection, but not in the orbital angular momenta. In the partial-wave analysis we are interested in a finite number of the lowest angular momentum states, corresponding to any of the possible schemes. Working with a finite number of 3-particle angular momentum states in each of these schemes we have to satisfy a consistency requirement that the few states, which are used for the dynamical assumption, are also the dominant one when we look at them in the πN mass spectra. However, the πN spectra do not provide a very sensitive test, because they do not change very much if we choose a different angular momentum for the production of the N^*, providing we assume N^* with its quantum numbers, mass, and the width. The πN spectra are therefore not very good tools for deciding which is the most important partial wave, if we work with the N^* model. On the other hand, these spectra are quite sensitive to the dynamical assumption on the radial part of the amplitude. This is so, because the subenergy of the πN subsystem is the same variable which we use for the mass of the N^* and at which we look in the πN mass spectrum. Therefore we only require that the πN spectra are compatible with the N^* assumption, and we use the $\pi\pi$ spectrum as a tool for finding the most dominant final angular momentum state in the set of states of the $(\pi\pi)N$ scheme.

B. $\pi^-p \to \pi^-\pi^+n$ at 430 MeV

In this section we present several details of our partial-wave analysis on the example of $\pi^-p \to \pi^-\pi^+n$ at 430 MeV. There are two reasons for concentrating on this process. First of all, the initial energy of this process is the lowest one which we will consider; thus it is the most favorable case for making an assumption on the radial part as proportional to the centrifugal-barrier factors. Secondly, the $\pi\pi$ mass spectrum, which is the main point of our interest in the partial-wave analysis, is known[21] to have a definite peak at the right-hand side of the $\pi\pi$ spectrum. We discuss a possible explanation of this peak by eliminating several hypotheses within our partial-wave analysis.

The initial angular momentum states at 430 MeV are the following, according to results from πN phase-shift analysis shown on Figs. 3 and 4:

$$\begin{aligned} &S_{31}, P_{11} \quad \text{for} \quad J=\tfrac{1}{2}; \\ &D_{31}, D_{33} \quad \text{for} \quad J=\tfrac{3}{2}. \end{aligned} \tag{18}$$

In the final state, if we work with a state $|JL_3Sl_3\sigma_3\rangle$ of the $(\pi\pi)N$ scheme, we shall consider the following lowest angular momentum states:

$$\begin{aligned} &|\tfrac{1}{2}\,0\,\tfrac{1}{2}\,0\,0\rangle,\ |\tfrac{1}{2}\,1\,\tfrac{1}{2}\,0\,0\rangle, \quad \text{for} \quad J=\tfrac{1}{2}, \\ &|\tfrac{3}{2}\,1\,\tfrac{1}{2}\,0\,0\rangle, \quad \text{for} \quad J=\tfrac{3}{2}. \end{aligned} \tag{19}$$

By the "lowest state" we mean a state $|JL_3Sl_3\sigma_3\rangle$ such that $J\leqslant\frac{3}{2}$, $L_3=0$ or 1, and $l_3=0$.

As a dynamical model we assume the N^* production in the S, P, and D waves. Here, S, P, D means that either L_1 or L_2, in the second unit operator, is equal to 0, 1, 2. We always assume that either $l_1=1$, or $l_2=1$, in the second unit operator. Now we can use parity and the total angular momentum conservation, to restrict the number of transitions between the initial states [Eq. (18)] and the final states [Eq. (19)]. Because of the same conservation laws we can also restrict the possible dynamical models. Therefore, we shall consider transitions shown in Table I.

In the $(\pi N)\pi$ scheme we can have in the final state either $|JL_2Sl_2\sigma_2\rangle$ or $|JL_1Sl_1\sigma_1\rangle$, and we shall consider transitions which are compatible with the same initial states as in Table I. These transitions are shown in Table II. The final states in Table II are the lowest ones in the sense that $J\leqslant\frac{3}{2}$, and L_1, or L_2 are equal to 0, 1, 2. Again we have either $l_1=1$, or $l_2=1$, to maintain the N^* assumption.

Now we can start our partial-wave analysis by trying

TABLE I. Partial-wave transitions for $\pi^-p \to \pi^-\pi^+n$ and $\pi^-p \to \pi^-\pi^0p$. The final states are classified in the $(\pi\pi)N$ scheme.

No.	Initial state	Final state	Isospin	Dynamical model
1	S_{31}	$\|\frac{1}{2}\,1\,\frac{1}{2}\,0\,0\rangle$	$\frac{3}{2}$	D-wave production of N^*
2	P_{11}	$\|\frac{1}{2}\,0\,\frac{1}{2}\,0\,0\rangle$	$\frac{1}{2}$	P-wave production of N^*
3	D_{13}	$\|\frac{3}{2}\,1\,\frac{1}{2}\,0\,0\rangle$	$\frac{1}{2}$	S-wave production of N^*
4				D-wave production of N^*
5	D_{33}	$\|\frac{3}{2}\,1\,\frac{1}{2}\,0\,0\rangle$	$\frac{3}{2}$	S-wave production of N^*
6				D-wave production of N^*

[21] J. Kirz, J. Schwartz, and D. Tripp, Phys. Rev. **130**, 2481 (1963); J. Kirz, Lawrence Radiation Laboratory Report No. UCRL-10720, 1963 (unpublished).

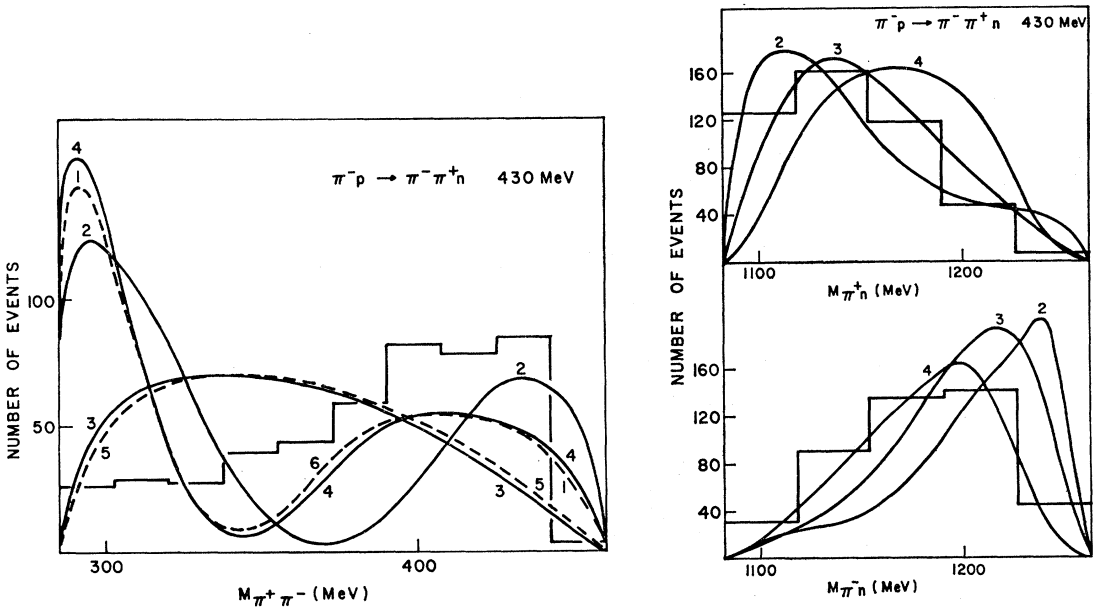

FIG. 5. (a) $\pi^+\pi^-$ mass spectra for transitions of Table I, taken separately. The experimental data (463 events) are from Kirz *et al.* (Ref. 21). (b) π^+n and π^-n spectra for transitions 2, 3, and 4 of Table II, taken separately. The experimental data (463 events) are from Kirz *et al.* (Ref. 21).

one of the transitions from Table I or II, taken separately. We ask whether any of them can explain all data on $\pi^+\pi^-$ and πN mass spectra. Our results are shown in Figs. 5(a) and 5(b). We see that the choice of transition has a larger effect on the $\pi^+\pi^-$ spectrum than on the πN spectra. The *shape* of the calculated $\pi^+\pi^-$ spectrum varies significantly, while the shape of the πN spectra is quite stable and roughly agrees with the experimental data. The agreement of the πN spectra is not surprising, because it is mainly due to the assumption of the N^* production. From Fig. 5(a) we see that none of the separate transitions can explain the $\pi^+\pi^-$ spectrum, which is the crucial test in our analysis. All of the curves have a pronounced peak at the left-hand side of the $\pi^+\pi^-$ spectrum.

The next step is to try a superposition of several transitions. Because of the orthogonality of the initial angular momentum states, there is only a small number of interesting superpositions which could remove the peak from the left-hand side of the $\pi^+\pi^-$ spectrum. Interference in the formula for mass distribution can occur only among those transitions which have the same initial state. Thus, we can superpose the following transitions: 3 and 4, or 5 and 6. The result of superposing 3 and 4 is shown in Fig. 6, and a similar result can be obtained by adding 5 and 6. We see that agreement with the experimental data is still not obtained and we make it even worse if we add another transition because each of them has a definite peak at the left-hand side of the $\pi^+\pi^-$ spectrum. Also, we do not obtain a better agreement by including some higher transitions corresponding to $J>\frac{3}{2}$, because they do not interfere with the previous one.

Thus, working with a finite number of angular momentum states and with the dynamical model of the N^* production, we can not explain all mass spectra of

TABLE II. Partial-wave transitions for $\pi^- p \rightarrow \pi^-\pi^+ n$ and $\pi^- p \rightarrow \pi^-\pi^0 p$. The final states are classified in the $(\pi N)\pi$ scheme.

No.	Initial state	Final state	Isospin	Dynamical model
1	S_{31}	$\lvert\frac{1}{2}\,2\,\frac{3}{2}\,1\,\frac{1}{2}\rangle$	$\frac{3}{2}$	D-wave production of N^*
2	P_{11}	$\lvert\frac{1}{2}\,1\,\frac{3}{2}\,1\,\frac{1}{2}\rangle$	$\frac{1}{2}$	P-wave production of N^*
3	D_{13}	$\lvert\frac{3}{2}\,0\,\frac{3}{2}\,1\,\frac{1}{2}\rangle$	$\frac{1}{2}$	S-wave production of N^*
4	D_{13}	$\lvert\frac{3}{2}\,2\,\frac{3}{2}\,1\,\frac{1}{2}\rangle$	$\frac{1}{2}$	D-wave production of N^*
5	D_{33}	$\lvert\frac{3}{2}\,0\,\frac{3}{2}\,1\,\frac{1}{2}\rangle$	$\frac{3}{2}$	S-wave production of N^*
6	D_{33}	$\lvert\frac{3}{2}\,2\,\frac{3}{2}\,1\,\frac{1}{2}\rangle$	$\frac{3}{2}$	D-wave production of N^*

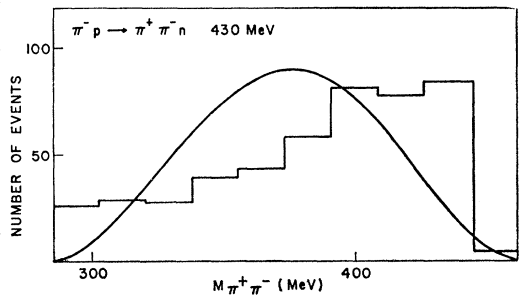

FIG. 6. $\pi^+\pi^-$ mass spectrum for the superposition of transitions 2 and 3 from Table I, in the ratio 1:5. The experimental data (463 events) are from Kirz *et al.* (Ref. 21).

TABLE III. Partial-wave transitions for $\pi^-p \to \pi^-\pi^+n$ and $\pi^-p \to \pi^-\pi^0p$. The final states are classified in the $(\pi\pi)N$ scheme.

No.	Initial state	Final state	Isospin	Dynamical model
2	P_{11}	$\|\frac{1}{2}0\frac{1}{2}00\rangle$	$\frac{1}{2}$	P-wave production of N^*
2′	P_{11}	$\|\frac{1}{2}0\frac{1}{2}00\rangle$	$\frac{1}{2}$	S-wave production of σ

process $\pi^-p \to \pi^-\pi^+n$ at 430 MeV. It will be seen, in the following sections, that the above conclusion is limited to the production of $\pi^-\pi^+n$ in the region of 400 MeV.

To explain the right-hand peak of the experimental data for the $\pi^+\pi^-$ spectrum at 430 MeV, we have to assume that there is at least one more transition besides those in Table I. That transition has to have the same initial state, so it can interfere with a transition from Table I. We have chosen the initial state to be the P_{11}, because according to Figs. 3 and 4 this initial state is the most important one at the energy around 400 MeV. Restricting ourselves to the initial state P_{11}, we have only one possible transition if we assume for the dynamical model only N^* production. Another transition with the same initial state, and incidently with the same final state, can be proposed if we allow the production of σ. We can then superpose two transitions, shown in Table III in the $(\pi\pi)N$ scheme. In the $(\pi N)\pi$ scheme we also have two unique transitions, if we restrict the initial state to be the P_{11}. They are shown in Table IV.

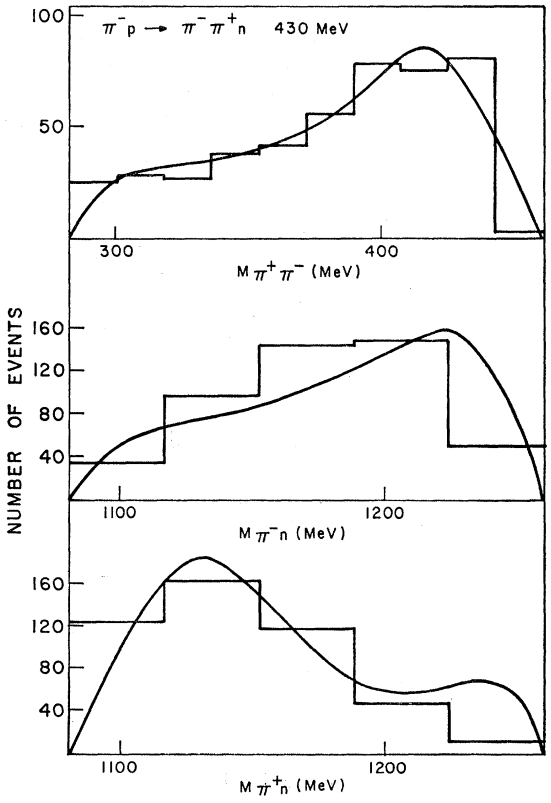

FIG. 7. $\pi^+\pi^-$, π^-n, and π^+n mass spectra for the superposition of transitions 2 and 2′ from Tables III and IV, in the ratio $1:(-0.1i)$. The experimental data (463 events) are from Kirz *et al.* (Ref. 21).

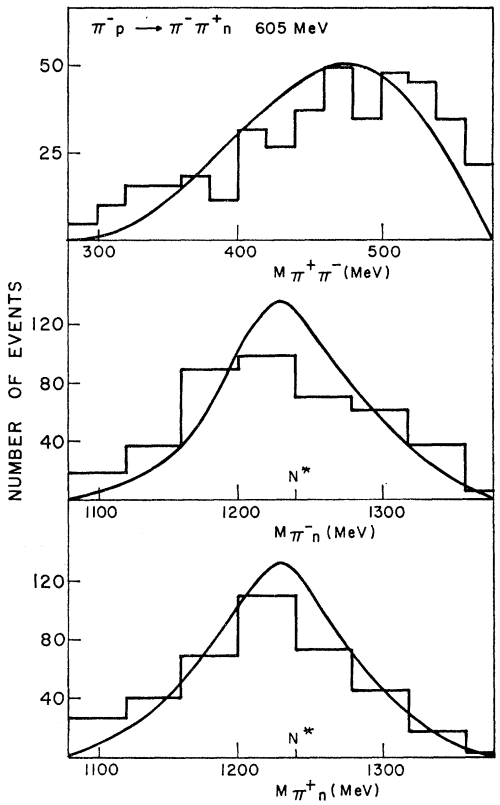

FIG. 8. $\pi^+\pi^-$, π^-n, and π^+n mass spectra for the superposition of transitions 3 and 4 from Tables I and II, in the ratio 1:5. The experimental data (383 events) are from Kirz *et al.* (Ref. 21).

Assuming that both transitions 2 and 2′ take place, we can explain all mass spectra of the process $\pi^-p \to \pi^-\pi^+n$ at 430 MeV. Our results are shown in Fig. 7. The second transition 2′ has to be taken with the coefficient $-0.1i$. To interpret this coefficient see Ref. 22.

Having obtained an agreement between our curves and all experimental data, we stop our analysis. It

TABLE IV. Partial-wave transition for $\pi^-p \to \pi^-\pi^+n$ and $\pi^-p \to \pi^-\pi^0p$. The final states are classified in the $(\pi N)\pi$ scheme.

No.	Initial state	Final state	Isospin	Dynamical model
2	P_{11}	$\|\frac{1}{2}1\frac{3}{2}1\frac{1}{2}\rangle$	$\frac{1}{2}$	P-wave production of N^*
2′	P_{11}	$\|\frac{1}{2}1\frac{3}{2}1\frac{1}{2}\rangle$	$\frac{1}{2}$	S-wave production of σ

[22] The coefficient we put in front of our radial part does not represent the ratio of amplitudes. It contains many other buried factors, because we have only extracted the centrifugal barrier factors [Eq. (15)] and the propagator [Eq. (16)]. To *estimate* the ratio of amplitudes we multiply our coefficient by an average value of centrifugal barrier factors and correct it by the effect of different mass, width, and spin of resonances. In the case of σ and N^* in π^-p scattering at 430 MeV, instead of 0.1 we get an effective factor 4.56.

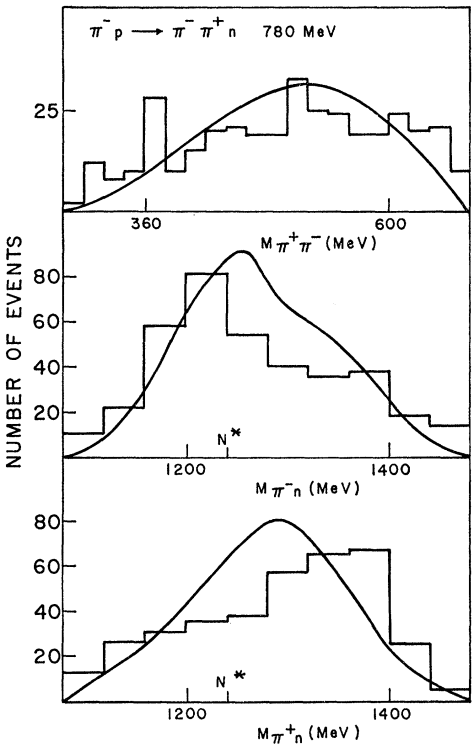

FIG. 9. $\pi^+\pi^-$, $\pi^- n$, and $\pi^+ n$ mass spectra for the superposition of transitions 3 and 4 from Tables I and II, in the ratio 1:5. The experimental data (350 events) are from Kirz *et al.* (Ref. 21).

could be carried further to obtain a better fit, if we had a more detailed knowledge about the radial part of the T matrix. At present, we stop our analysis on a minimum number of transitions which are compatible with all experimental data. We are trying to restrict the number of transitions to a minimum, in order to minimize the number of free parameters which arise because of our poor knowledge of the radial part of the T matrix.

C. $\pi^- p \longrightarrow \pi^-\pi^+ n$ and $\pi^- p \longrightarrow \pi^-\pi^0 p$

This section deals with the partial-wave analysis in the following processes: (i) $\pi^- p \longrightarrow \pi^-\pi^+ n$, at 605 MeV, 780 MeV, and 905 MeV, (ii) $\pi^- p \longrightarrow \pi^-\pi^0 p$, at 450 MeV and 905 MeV. These processes we can explain by assuming only N^* production. σ cannot be produced in processes (ii) because of the isospin, and it is not expected to be produced in the processes (i) which are at energies of 600 MeV and higher.

All processes (i) and (ii) can be explained by an appropriate superposition of transitions from Tables I or II. Our results are shown in Figs. 8, 9, 10, 11(b), and 12. All processes (i) and the last process of (ii) can be explained by superposing transitions 3 and 4. We concentrate only on the initial state D_{13}, because above 600 MeV this is the most dominant state. Another transition could be included but only at the expense of adding a new parameter. Transitions 3 and 4 were taken with the ratio 1:5 at 605 MeV and 780 MeV, and with the ratio 1:3 at 905 MeV. These ratios[22] were chosen because of the centrifugal-barrier factor in the expression for the radial part of the T matrix. That factor is approximately 1/4.3 at 650 MeV and 1/3.5 at 905 MeV. Thus, by taking the above ratios we allow roughly equal probability for both transitions 3 and 4.

The first process of (ii) is in the energy region, where the most important initial states are P_{11} and D_{13}. Thus, we should consider transitions 2, 3, and 4. If we assume only one of these transitions, or a superposition of 3 and 4 with the ratio 1:5, then we get results shown in Fig. 11(a). By including all three transitions in the ratio 1:1:5, we get curves shown in Fig. 11(b). It should be noticed that the above ratio[22] discriminates against the transition 2 which has the P-wave centrifugal-barrier factor. Because of that the result for the $\pi\pi$ spectrum obtained by superposing 3 and 4 is similar when 2, 3, and 4 are taken in the ratio 1:1:5. In that way we can allow the presence of the initial state P_{11} and get a reasonable agreement with all experimental data shown in Fig. 11(b), working only with the N^* production. At a

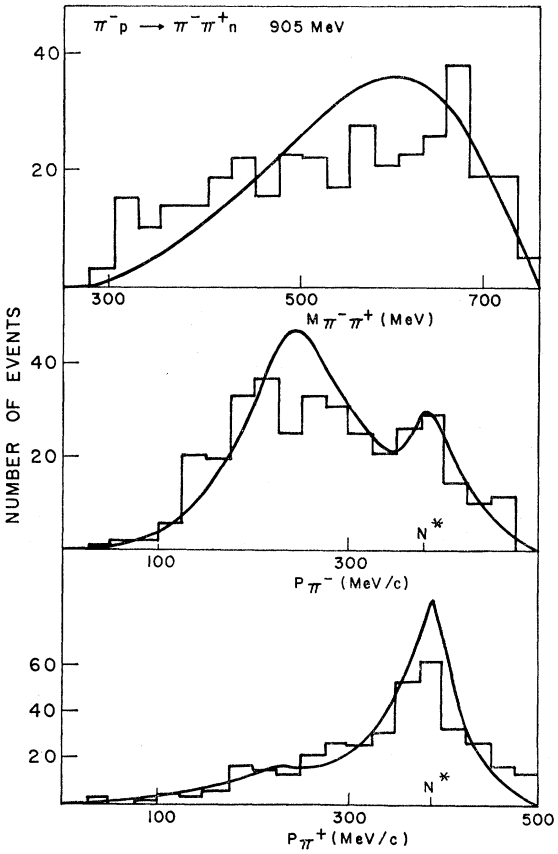

FIG. 10. $\pi^+\pi^-$ mass spectrum and center-of-mass momentum distribution for π^- and π^+, calculated for the superposition of transitions 3 and 4 from Tables I and II, in the ratio 1:3. The experimental data (354 events) are from E. Pickup, D. K. Robinson, E. O. Salant, F. Ayer, and B. A. Munir [Phys. Rev. **132**, 1819 (1963)].

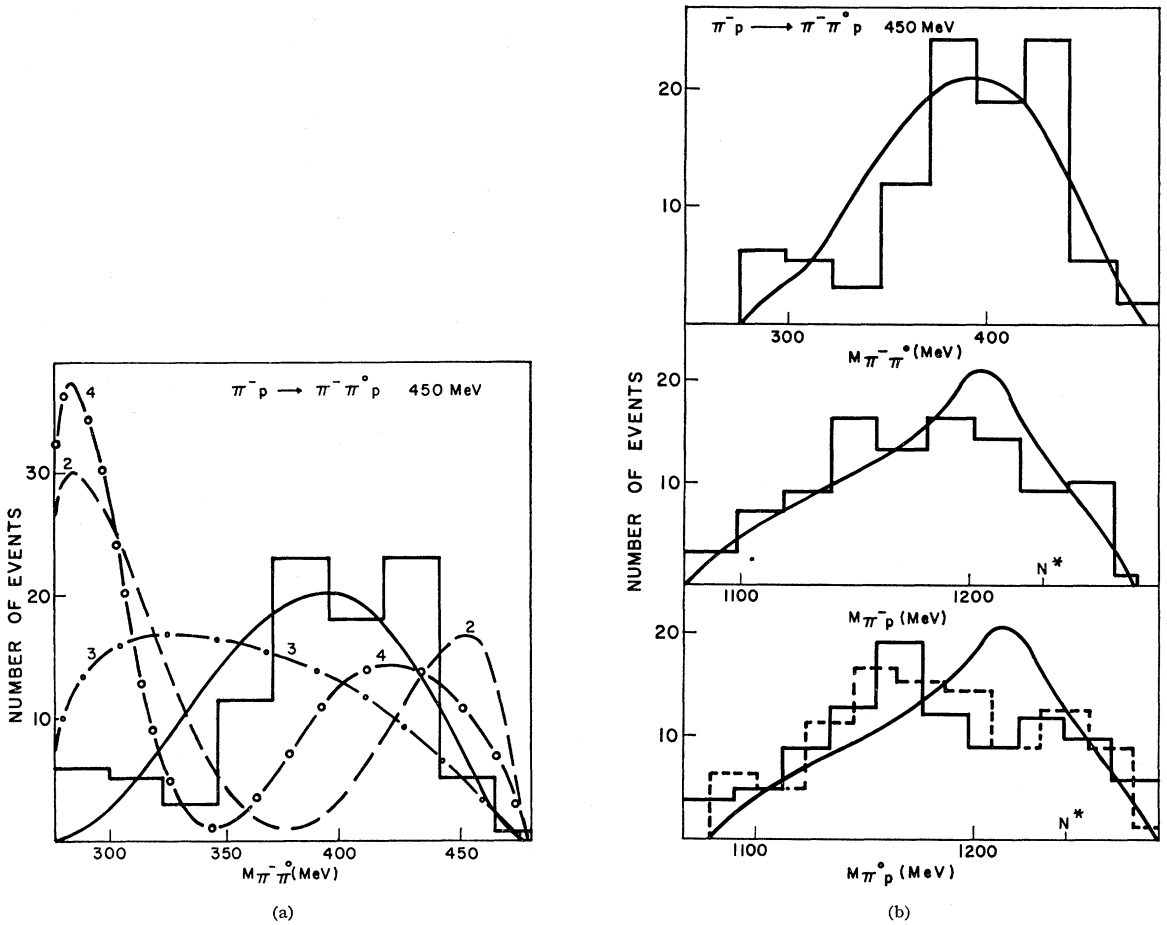

FIG. 11. (a) $\pi^-\pi^0$ mass spectra for transitions 1, 2, and 3 from Table I, taken separately, and for the superposition of 2 and 3 in the ratio 1:5. The experimental data (100 events) are from H. Martin (private communication), and Ref. 17. (b) $\pi^-\pi^0$, $\pi^- p$, and $\pi^0 p$ mass spectra for the superposition of transitions 2, 3, and 4 from Tables I and II, in the ratio 1:1:5. The experimental data (100 events) are from H. Martin (private communication) and Ref. 17—solid curve, and from C. P. Poirer, C. A. Tilger, E. D. Alyea, Jr., J. H. Martin, Jr., J. I. Rhode, and J. H. Scandrett [Phys. Rev. 148, 1311 (1966)]—dashed curve.

similar energy, in the companion process $\pi^- p \longrightarrow \pi^-\pi^+ n$, we had to introduce the σ production, which was plausible in the case of that process. In the present case, σ is excluded by the isospin. Our agreement in Figs. 7 and 11(b) indicates some consistency of the assumed dynamical model.

D. $\pi^+ p \longrightarrow \pi^0\pi^+ p$ and $\pi^+ p \longrightarrow \pi^+\pi^+ n$

This section deals with processes (iii) $\pi^+ p \longrightarrow \pi^0\pi^+ p$ at 600 MeV and 820 MeV, (iv) $\pi^+ p \longrightarrow \pi^+\pi^+ n$ at 600 MeV. These processes have total isospin equal $\frac{3}{2}$; therefore we consider the following initial states:

$$\begin{aligned} &S_{31}, && \text{for } J=\tfrac{1}{2} \\ &P_{33}, D_{33}, && \text{for } J=\tfrac{3}{2}. \end{aligned} \tag{20}$$

We have not included P_{31} because, according to Fig. 4, this initial state is of smaller importance than the states of Eq. (20).

For the dynamical model we again assume only N^* production. There is no possible σ production because of the isospin.

Working with states of the $(\pi\pi)N$ scheme we shall consider transitions shown in Table V. In the $(\pi N)\pi$ scheme we shall deal with the same initial states, and consider transitions given in Table VI. As in the previous sections, we start our partial-wave analysis by assuming separately only one of the above transitions. Our results for $\pi^+\pi^0$ mass distribution are shown on Fig. 13. Again

TABLE V. Partial-wave transitions for $\pi^+ p \longrightarrow \pi^0\pi^+ p$ and $\pi^+ p \longrightarrow \pi^+\pi^+ n$. The final states are classified in the $(\pi\pi)N$ scheme.

No.	Initial state	Final state	Isospin	Dynamical model
1	S_{31}	$\lvert\frac{1}{2}\,1\,\frac{1}{2}\,0\,0\rangle$	$\frac{3}{2}$	D-wave production of N^*
5	D_{33}	$\lvert\frac{3}{2}\,1\,\frac{1}{2}\,0\,0\rangle$	$\frac{3}{2}$	S-wave production of N^*
6				D-wave production of N^*
7	P_{33}	$\lvert\frac{3}{2}\,2\,\frac{1}{2}\,0\,0\rangle$	$\frac{3}{2}$	P-wave production of N^*
8				F-wave production of N^*

TABLE VI. Partial-wave transitions for $\pi^+p \to \pi^0\pi^+p$ and $\pi^+p \to \pi^+\pi^+n$. The final states are classified in the $(\pi N)\pi$ scheme.

No.	Initial state	Final state	Isospin	Dynamical model
1	S_{31}	$\left\|\frac{1}{2}\,2\,\frac{3}{2}\,1\,\frac{1}{2}\right\rangle$	$\frac{3}{2}$	D-wave production of N^*
5	D_{33}	$\left\|\frac{3}{2}\,0\,\frac{3}{2}\,1\,\frac{1}{2}\right\rangle$	$\frac{3}{2}$	S-wave production of N^*
6	D_{33}	$\left\|\frac{3}{2}\,2\,\frac{3}{2}\,1\,\frac{1}{2}\right\rangle$	$\frac{3}{2}$	D-wave production of N^*
7	P_{33}	$\left\|\frac{3}{2}\,1\,\frac{3}{2}\,1\,\frac{1}{2}\right\rangle$	$\frac{3}{2}$	P-wave production of N^*
8	P_{33}	$\left\|\frac{3}{2}\,3\,\frac{3}{2}\,1\,\frac{1}{2}\right\rangle$	$\frac{3}{2}$	F-wave production of N^*

we notice that none of the separate transitions can explain the experimental data for the $\pi^+\pi^0$ spectrum. Therefore we have to consider a superposition of several transitions. At 600 MeV we have in the initial state only S_{31} and D_{33} and therefore we superspose transitions 1, 5, and 6. Our results for the first process of (iii) and (iv) are shown in Figs. 14 and 15, correspondingly. We have taken transitions 1, 5, and 6 in the ratio 3:1:5.

Considering the process $\pi^+p \to \pi^0\pi^+p$ at 820 MeV, we should include, besides 1, 5, and 6, transitions 7 and 8. The best fit is shown in Fig. 16, and it was obtained

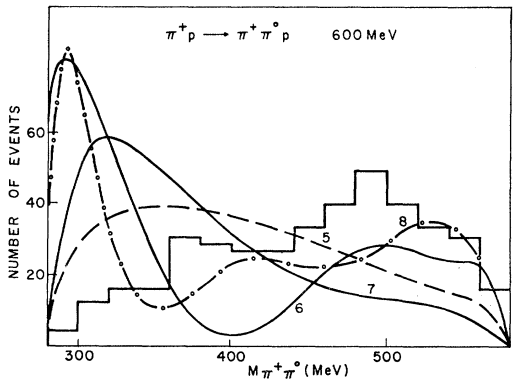

FIG. 13. $\pi^+\pi^0$ mass spectra for transitions 1, 5, 6, 7, and 8 from Table V, taken separately. The experimental data (418 events) are from P. C. A. Newcomb [Phys. Rev. **132**, 1238 (1963)].

from transitions 5, 6, 7, and 8 taken in the ratio 1:5:(−4):(−10). We have not included the transition 1, because any amount of it produced disagreement with the experimental data. That feature is illustrated in Fig. 17, where we show two curves, one for the

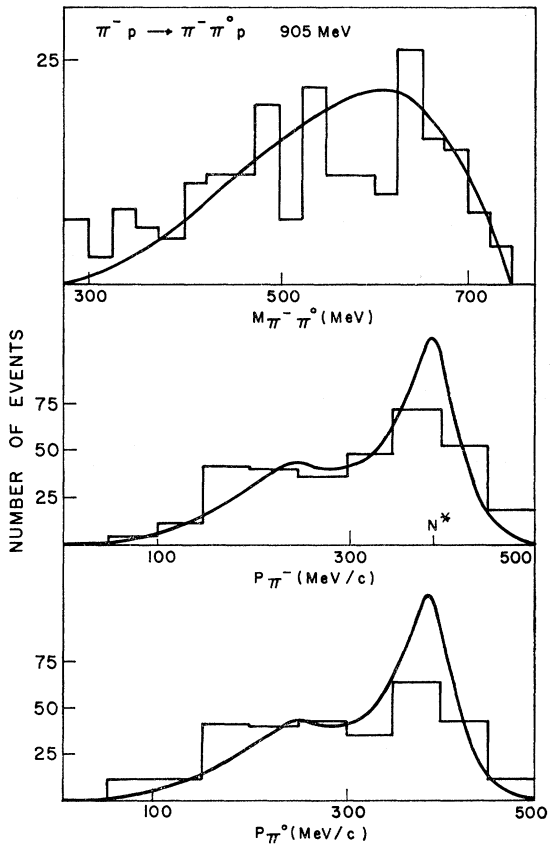

FIG. 12. $\pi^-\pi^0$ mass spectrum and center-of-mass momentum distribution for π^- and π^0, calculated for the superposition of transitions 3 and 4 from Tables I and II, in the ratio 1:3. The experimental data (216 events) are from E. Pickup, D. K. Robinson, E. G. Salant, F. Ayer, and B. A. Munir [Phys. Rev. **132**, 1819 (1963)].

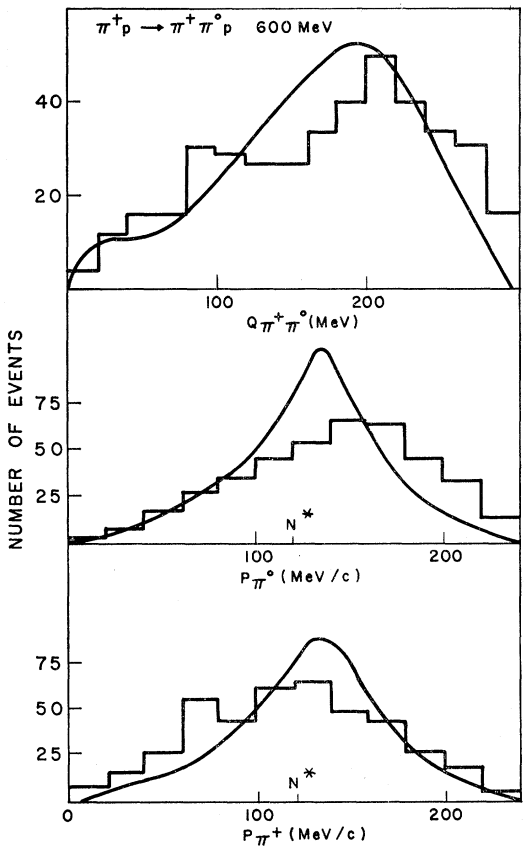

FIG. 14. $\pi^+\pi^0$ mass spectrum ($Q_{\pi^+\pi^0}=M_{\pi^+\pi^0}-2m_\pi$) and center-of-mass momentum distribution for π^0 and π^+, calculated for the superposition of transitions 1, 5, and 6 from Tables V and VI, in the ratio 3:1:5. The experimental data (418 events) are from P. C. A. Newcomb [Phys. Rev. **132**, 1238 (1963)].

superposition of 5 and 6 with the ratio 1:5, another for the superposition of 1, 5, and 6 in the ratio 3:1:5. The factor 3 in the front of the transition 1 is to balance the centrifugal-barrier factor in the final state.[22] In our formulas we do not include any centrifugal-barrier factor for the initial state.

E. Angular Distributions

We have also calculated the center-of-mass angular distributions for these superpositions of the considered transitions, for which we obtained the best fit for the mass spectra. We present only a few examples of angular

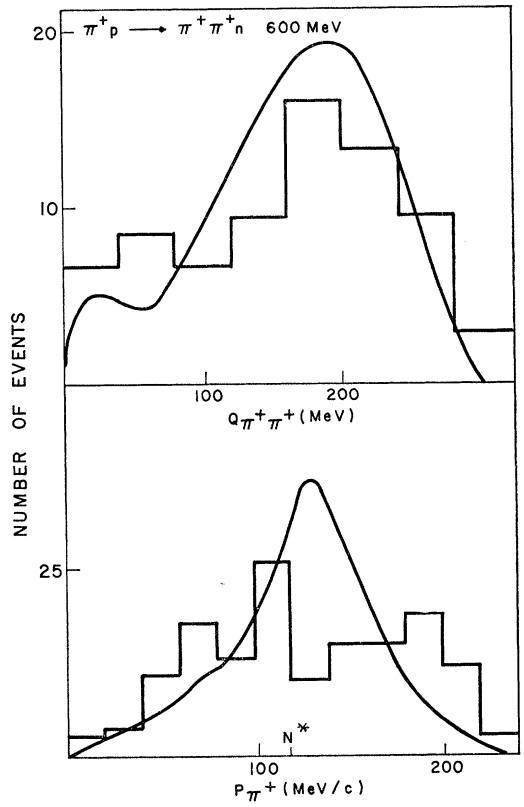

FIG. 15. $\pi^+\pi^+$ mass spectrum and center-of-mass momentum distribution for π^+, calculated for the superposition of transitions 1, 5, and 6 from Tables V and VI, in the ratio 3:1:5. The experimental data (75 events) are from P. C. A. Newcomb [Phys. Rev. **132**, 1238 (1963)].

distributions to illustrate the shape[23] of curves which we have obtained. In Fig. 18 we show results for the following processes: $\pi^-p \rightarrow \pi^-\pi^+n$ at 905 MeV; $\pi^-p \rightarrow \pi^-\pi^0p$ at 450 MeV, and 905 MeV. In Fig. 19 we have angular distributions for $\pi^+p \rightarrow \pi^0\pi^+p$ at 600 MeV; $\pi^+p \rightarrow \pi^+\pi^+n$ at 600 MeV. The agreement with experimental data is reasonable in some cases, but not satisfactory in all of them. Results for angular distributions are very sensitive to all interference effects between any of the considered transitions. In our analysis we have taken only the minimum number of transitions, in order to minimize the number of free parameters. Thus it is not surprising that our results for angular

[23] The symmetric shape of our curves for the angular distribution is caused by our simplified assumption about the radial part.

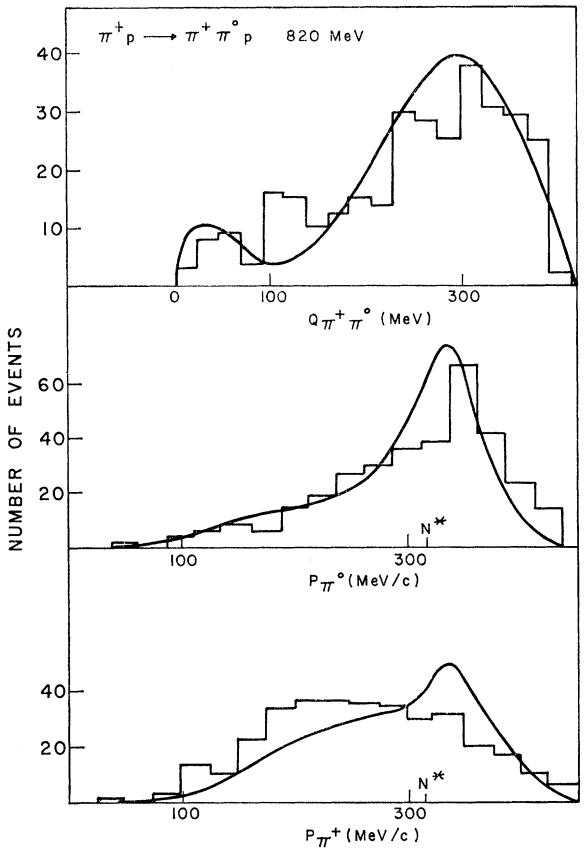

FIG. 16. $\pi^+\pi^0$ mass spectrum and center-of-mass momentum distribution for π^0 and π^+, calculated for the superposition of transitions 5, 6, 7, and 8 from Tables V and VI, in the ratio 1:5:(−4):(−10). The experimental data (347 events) are from R. Barloutaud, J. Heughebart, A. Leveque, C. Louedec, J. Meyer, and D. Tycho [Nuovo Cimento **27**, 238 (1963)].

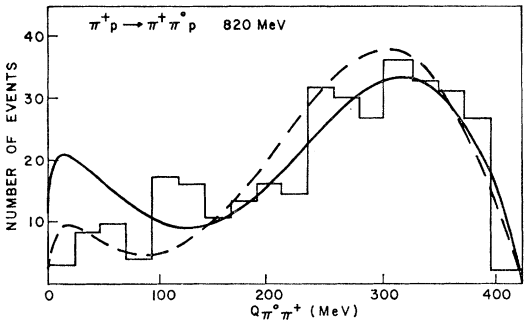

FIG. 17. $\pi^+\pi^0$ mass spectrum for the superposition of transitions 5 and 6 in the ratio 1:5—dashed line, and for the superposition of 1, 5, and 6 in the ratio 3:1:5—solid line. The experimental data (347 events) are from R. Barloutaud, J. Heughebart, A. Leveque, C. Louedec, J. Meyer, and D. Tycho [Nuovo Cimento **27**, 238 (1963)].

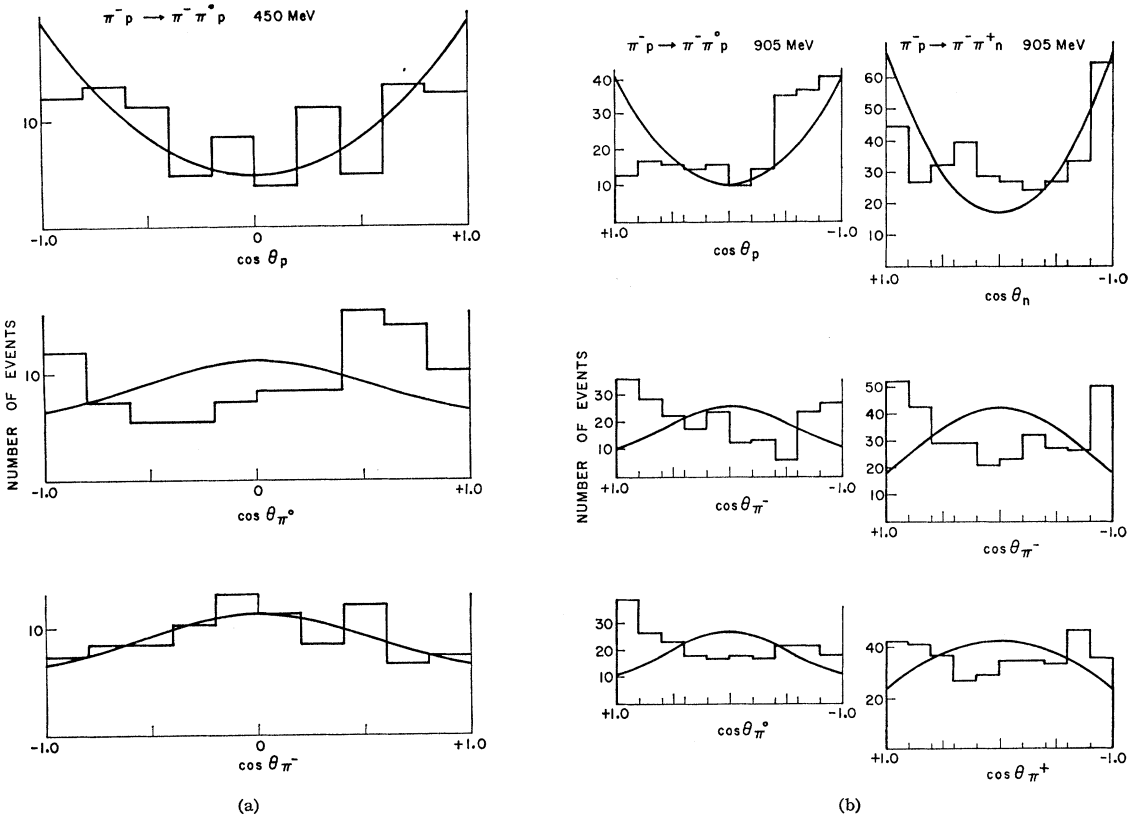

FIG. 18. The center-of-mass angular distributions for transitions described in Figs. 10, 11(b), and 12, correspondingly.

distributions only roughly agree with the experimental data.

F. Conclusions

To conclude our partial-wave analysis of $\pi N \to \pi\pi N$ we summarize the main results.

(1) The $\pi\pi$ mass spectrum is a *sensitive test* of a particular choice of the partial-wave transition. At the same time this spectrum is rather insensitive to a definite form of the radial part of the T matrix, if we work only with the N^* production. Therefore, the $\pi\pi$ spectrum is a good tool for partial-wave analysis, even with an approximate dynamical model.

(2) All mass spectra, and the center-of-mass angular distributions can be explained by the following transitions. We use the $(\pi\pi)N$ scheme to denote the final angular momentum state.

(a) $\pi^- p \to \pi^- \pi^+ n$ below 500 MeV:
$P_{11} \to |\frac{1}{2}\,0\,\frac{1}{2}\,0\,0\rangle_{I=1/2}$ P-wave production of N^* and S-wave production of σ.

(b) $\pi^- p \to \pi^- \pi^0 p$ below 500 MeV:
$P_{11} \to |\frac{1}{2}\,0\,\frac{1}{2}\,0\,0\rangle_{I=1/2}$ P-wave production of N^*,
$D_{13} \to |\frac{3}{2}\,1\,\frac{1}{2}\,0\,0\rangle_{I=1/2}$ S- and D-wave production of N^*.

(c) $\pi^- p \to \pi^- \pi^+ n$ and $\pi^- p \to \pi^- \pi^0 p$, 600–900 MeV:
$D_{13} \to |\frac{3}{2}\,1\,\frac{1}{2}\,0\,0\rangle_{I=1/2}$ S- and D-wave production of N^*.

(d) $\pi^+ p \to \pi^0 \pi^+ p$ and $\pi^+ p \to \pi^+ \pi^+ n$ around 600 MeV:
$S_{31} \to |\frac{1}{2}\,1\,\frac{1}{2}\,0\,0\rangle_{I=3/2}$ D-wave production of N^*,
$D_{33} \to |\frac{3}{2}\,1\,\frac{1}{2}\,0\,0\rangle_{I=3/2}$ S- and D-wave production of N^*.

(e) $\pi^+ p \to \pi^0 \pi^+ p$, around 800 MeV:
$D_{33} \to |\frac{3}{2}\,1\,\frac{1}{2}\,0\,0\rangle_{I=3/2}$ S- and D-wave production of N^*,
$P_{33} \to |\frac{3}{2}\,2\,\frac{1}{2}\,0\,0\rangle_{I=3/2}$ P- and F-wave production of N^*.

VII. COMPARISON WITH OTHER FORMALISMS AND FINAL REMARKS

Pion production processes $\pi N \to \pi\pi N$ have been studied by many authors with the use of the isobar model or a model closely related to it. We recall papers of Lindenbaum and Sternheimer,[15] Bergia, Bonsignori, and Stanghellini,[16] Olsson and Yodh,[17] Thurnauer,[10] and Deler and Valladas.[11] In the following there are a few remarks pointing out some differences between their approach and ours.

Lindenbaum and Sternheimer[15] assumed that the isobar was always produced in the S wave and decayed

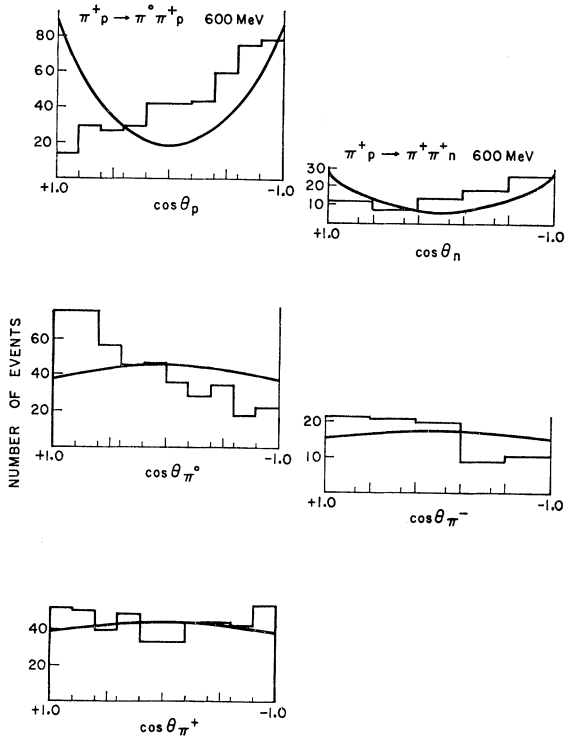

FIG. 19. The center-of-mass angular distributions for transitions described in Figs. 14 and 15.

in the S wave too. Furthermore, they assumed that the interference between the two diagrams, corresponding to the simultaneous production of N^*, could be neglected. The results they obtained for the mass spectra were roughly in agreement with experiment.

It was pointed out by Bergia, Bonsignori, and Stanghellini[16] that one should include the interference between the two diagrams, but they found that the effect of doing so was to obtain a pronounced dip in the mass distribution, which was not seen experimentally.

That disturbing feature was removed by Olsson and Yodh,[17] who showed that the inclusion of the correct P-wave decay of the πN resonance, and the requirement of Bose statistics rectified the spectra, and they obtained quite good agreement with experiment. Their model accounts for the $\pi\pi$ mass distribution in most charge states, but not for the $\pi^+\pi^-$ spectrum obtained in the experiment of Kirz *et al.*[21]

A general, relativistic, and unitary scheme, using the canonical base of Macfarlane,[4] was formulated by Thurnauer.[10] However, in his calculations of the mass spectra of the process $\pi^-p \to \pi^-\pi^+n$, there is assumed only the S-wave production of any resonance, and the P_{11} or D_{13} initial states. His assumption about the final S-wave production remains for all incident energies in the range 212–780 MeV.

Recently, Deler and Valladas[11] have formulated a practical, relativistic scheme using the isobar model. Their formalism is very similar to ours, but they differ from us by allowing a mixture of two states from different complete sets. These two states have numerically the same quantum numbers, but they belong to two independent set of states. Deler and Valladas[11] have calculated the mass spectra for $\pi^+p \to \pi^+\pi^0p$ at 510 MeV and 810 MeV. Their results are in some cases different from ours. The reason for this is that they calculated transitions which are essentially different from the ones considered by us. Their transitions are from a given initial angular momentum state to a superposition of an infinite number of the final 3-body angular momentum states, if one looks at them using only one complete set of states. We have selected one transition, or a superposition of a finite number of them. This was possible only because we have two unit operators for the 3-body angular momentum states. Our matrix element contains a given recoupling coefficient, and it enables us to distinguish easily between quite different shapes of the $\pi\pi$-mass spectra, corresponding to different transitions. We can select transitions, and superpose them in a systematic way, because our final states belong to only one complete set of states.

Concerning our calculations, we add the following remarks. Our partial-wave analysis employs a definite dynamical model, so its numerical results depend on this model. One can use our formulas for another input, because the formalism is written in such a way that it can be easily used for any form of the radial part of the T matrix. For example, we can put in our formulas a solution of the Faddeev equation, and get quantities which could be compared with the experimental data. We have not included any 3-body forces, which could easily be incorporated, although they imply much more lengthy expressions. Several details of calculations with the 3-body forces, in the separable Faddeev theory, are presented in the paper of Freedman, Lovelace, and Namyslowski.[2]

In our present partial-wave analysis, we did not saturate all possibilities of explaining the experimental data. We have rather pointed out some possible solutions which are compatible with all experimental data. Our aim was to explain several processes with the minimum number of transitions to minimize the number of free parameters. One could extend our analysis by including more transitions. In particular, one could include transitions with $I=\frac{1}{2}$ as well as $I=\frac{3}{2}$ when the π^-p scattering is considered. By doing so, one would improve the agreement with the experiment, but would introduce many more parameters. Our aim was to deal with the most dominant transitions and to present the basic idea of a systematic partial-wave analysis. If we achieve a better knowledge of the radial part of the T matrix from the Faddeev equation, then we shall be able to improve our analysis by including all transitions which could arise in a given process.

ACKNOWLEDGMENTS

The authors would like to thank Dr. C. Lovelace for suggesting these investigations and for many helpful discussions. Two of us (J. M. N. and M. S. K. R.) would like to thank Professor P. T. Matthews for his hospitality at the Imperial College, where this work was started, and the numerical calculations were done. One of us (J. M. N.) would like to acknowledge the hospitality of the Institute of Theoretical Physics, Stanford University, where the final version of the present paper was formulated.

APPENDIX A

In this Appendix we give an example of the quantity M introduced in Eq. (12) of Sec. IVA.

$$M_{\lambda_a\lambda_b}{}^{J\,j_\alpha m_\alpha \nu_\beta \nu_\gamma \lambda}{}_\alpha = \sum_I \Big[\sum_{T_\alpha} \Lambda_{IT_\alpha} \tilde{T}_{(\alpha,\alpha)}{}^{IT_\alpha} + \sum_{T_\alpha T_\beta} \Lambda_{IT_\alpha} V_{T_\beta I_\beta}{}^{IT_\alpha I_\alpha} \tilde{T}_{(\alpha,\beta)}{}^{IT_\beta} + \sum_{T_\alpha T_\gamma} \Lambda_{IT_\alpha} V_{T_\gamma I_\gamma}{}^{IT_\alpha I_\alpha} \tilde{T}_{(\alpha,\gamma)}{}^{IT_\gamma}\Big],$$

where $\tilde{T}_{(\alpha,\alpha)}{}^{IT_\alpha} = T_{\lambda_a\lambda_b}{}^{IT_\alpha J j_\alpha m_\alpha \nu_\beta \nu_\gamma \lambda_\alpha}(w_\alpha, W)$ is the radial part of the T matrix.

$$\tilde{T}_{(\alpha,\beta)}{}^{IT_\beta} = \tfrac{1}{2} \sum_{j_\beta m_\beta \mu_\alpha \mu_\beta \mu_\gamma} \left(\frac{p_\alpha q_\alpha}{w_\alpha}\right)^{1/2} \left(\frac{w_\beta}{p_\beta q_\beta}\right)^{1/2} \times (2j_\alpha+1)^{1/2}(2j_\beta+1)^{1/2}(-1)^{s_\beta-\mu_\beta+s_\gamma+\mu_\gamma} \times d_{m_\beta-\mu_\beta,\,m_\alpha-\lambda_\alpha}{}^{J}(\chi_\gamma)\, d_{m_\alpha,\nu_\beta\gamma}{}^{j_\alpha}(\theta_\alpha) d_{m_\beta,\mu_\gamma\alpha}{}^{j_\beta}(\theta_\beta) d_{\mu_\beta\nu_\beta}{}^{s_\beta}(\beta_{\beta\gamma}) \times d_{\mu_\gamma\nu_\gamma}{}^{s_\gamma}(\rho_\gamma)_{\mu_\alpha\lambda_\alpha}{}^{s_\alpha}(-\beta_{\alpha\gamma}) T_{\lambda_a\lambda_b}{}^{IT_\beta J j_\beta m_\beta \mu_\gamma \mu_\alpha \mu_\beta}(w_\beta, W).$$

$$\tilde{T}_{(\alpha,\gamma)}{}^{IT_\gamma} = \tfrac{1}{2} \sum_{j_\gamma m_\gamma \mu_\alpha \mu_\beta \mu_\gamma} \left(\frac{p_\alpha q_\alpha}{w_\alpha}\right)^{1/2} \left(\frac{w_\gamma}{p_\gamma q_\gamma}\right)^{1/2} \times (2j_\alpha+1)^{1/2}(2j_\gamma+1)^{1/2}(-1)^{s_\alpha-\lambda_\alpha+s_\beta+\lambda_\beta} \times d_{m_\alpha-\lambda_\alpha,\,m_\gamma-\mu_\gamma}{}^{J}(\chi_\beta)\, d_{m_\alpha,\nu_\beta\gamma}{}^{j_\alpha}(\theta_\alpha) d_{m_\gamma,\mu_\alpha\beta}{}^{j_\gamma}(\theta_\gamma) d_{\lambda_\alpha\mu_\alpha}{}^{s_\alpha}(\beta_{\alpha\beta}) \times d_{\nu_\beta\mu_\beta}{}^{s_\beta}(\rho_\beta) d_{\nu_\gamma\mu_\gamma}{}^{s_\gamma}(-\beta_{\gamma\beta}) T_{\lambda_a\lambda_b}{}^{IT_\gamma J j_\gamma m_\gamma \mu_\alpha \mu_\beta \mu_\gamma}(w_\gamma, W).$$

All angles are explained in Fig. 1 and in Appendix B.

APPENDIX B

In this Appendix we collect some kinematical formulas and give expressions for Wick[3] angles introduced in Fig. 1.

The magnitude of the 3-momentum $\mathbf{q}_\alpha$ of the particle α in the over-all center-of-mass frame is given by $q_\alpha = |\mathbf{q}_\alpha| = (2W)^{-1}\lambda(W^2, w_\alpha^2, m_\alpha^2)$, where λ is defined $\lambda(a,b,c) \equiv (a^2+b^2+c^2-2ab-2bc-2ca)^{1/2}$.

The magnitude of the 3-momentum $\mathbf{p}_\gamma$ of particles β, α in their rest frame is given by

$$p_\gamma = (2w_\gamma)^{-1}\lambda(w_\gamma^2, m_\alpha^2, m_\beta^2).$$

The Wick[3] angles, introduced in Fig. 1, can be calculated in terms of the total energy W and subenergies w_α, w_β, w_γ from the following expressions:

$$\cos\theta_\alpha = (4Ww_\alpha p_\alpha q_\alpha)^{-1}\big[(W^2-m_\alpha^2)(m_\gamma^2-m_\beta^2) + w_\alpha^2(w_\beta^2-w_\gamma^2)\big],$$

$$\cos\chi_\alpha = (4W^2 q_\beta q_\gamma)^{-1}\big[w_\beta^2 w_\gamma^2 + (W^2-m_\beta^2)w_\gamma^2 + (W^2-m_\gamma^2)w_\beta^2 - (W^2+2m_\alpha^2-m_\beta^2-m_\gamma^2)W^2 + m_\beta^2 m_\gamma^2\big],$$

$$\cos\beta_{\alpha\beta} = (4Ww_\gamma p_\gamma q_\alpha)^{-1}\big[(w_\gamma^2+m_\alpha^2-m_\beta^2) \times (W^2-w_\alpha^2+m_\alpha^2) - 2m_\alpha^2(W^2+w_\gamma^2-m_\gamma^2)\big],$$

$$\rho_\gamma = \beta_{\gamma\alpha}+\beta_{\gamma\beta}, \quad \rho_\beta = \beta_{\beta\alpha}+\beta_{\beta\gamma}.$$